*J. Am. Chem. Soc.* **2000,** *122,* 4483−4488

# The $CO_2$−NO van der Waals Complex and the Covalently Bonded $CO_2NO^-$ Anion: A Matrix-Isolation FTIR and Theoretical Study

**Mingfei Zhou,* Luning Zhang, and Qizong Qin**

*Contribution from the Laser Chemistry Institute, Fudan University, Shanghai, 200433, P.R. China*

*Received January 3, 2000*

**Abstract:** Laser ablation of transition metal targets with concurrent 11 K deposition of $NO/CO_2/Ar$ mixture produces $ON-CO_2$ van der Waals complex absorption at 1876.5 $cm^{-1}$ and three additional metal independent absorptions at 1713.6, 1495.8, and 1310.4 $cm^{-1}$. Based on isotopic substitution and theoretical calculations, these three bands are assigned to the antisymmetric $CO_2$ stretching, N−O stretching, and symmetric $CO_2$ stretching vibrations of the $CO_2NO^-$ anion. Our theoretical calculation results show that the $CO_2NO^-$ anion is a covalently bound molecule with coordination between the C and N atoms. The binding energy of the $CO_2NO^-$ with respect to $CO_2 + NO^-$ is estimated to be about 21−22 kcal/mol.

## Introduction

The nitric oxide molecule has one unpaired electron in the $2\pi^*$ orbital, which makes it more reactive than other diatomic molecules such as CO and $N_2$. The NO molecule can form a dimmer easily, which has been the subject of numerous theoretical[1] and experimental studies.[2] The carbon dioxide neutral dimmer has also been well studied, and its nonplanar $C_{2h}$ configuration has been determined.[3,4] van der Waals complexes of NO-X and $CO_2$-X (X = rare gas atoms, $H_2O$, CO, et al.) have received much attention in recent years.[5] To our knowledge, there is no report on the $CO_2$−NO complex.

Molecular ions derived from carbon dioxide, nitric oxide, and their clusters have been proven to participate in the chemistry of the terrestrial stratosphere and lower ionosphere,[6] and are potential intermediates in carbon dioxide and nitric oxide reduction processes. Both carbon dioxide and nitric oxide cluster anions have been intensively studied by experiment and by theoretical calculations.[7−15] The photoelectron spectra and vertical detachment energies of these cluster anions prepared by electron attachment have been measured in the gas phase.[7,12] The vibrational spectra of simple carbon dioxide and nitric oxide cluster anions were observed in rare gas matrices.[10,11,14,15] Studies of the clusters involving both $CO_2$ and NO units were focused on cations such as $NO^+(CO_2)_n$ ($n = 1-5$).[16] However, there is no report on the anions that contain both $CO_2$ and NO units up to now. The $CO_2NO^-$ anion is the simplest anion species involving both $CO_2$ and NO units and is isoelectronic with the neutral $N_2O_3$ molecule.

Laser ablation has proven to be an effective method to generate reaction intermediates and radicals for matrix isolation spectroscopic studies.[17] Bondybey first reported that the products of laser ablation can be trapped for leisurely investigation in low-temperature matrices.[18] Besides neutral species, laser ablation also produces electrons and abundant ions.[19−21] Recent works in Andrews' group[10,14,22,23] showed that metal-dependent as well as metal-independent anions can be formed via electron capture during condensation of laser-ablated metal atoms and electrons with small molecules. In this paper, we present the first experimental observation of the covalently bonded $CO_2NO^-$ anion produced by co-condensation of laser-ablated metal atoms and electrons with NO and $CO_2$ mixture in excess argon.

## Experimental and Computational Methods

The experimental setup for pulsed laser ablation and matrix infrared spectroscopic investigation is similar to that described previously.[24,25]

---

[1] See for example: East, A. L. L.; McKellar, A. R. W.; Watson, J. K. G. *J. Chem. Phys*. **1998**, *109*, 4378 and references therein.

[2] See for example: East, A. L. L. *J. Chem. Phys*. **1998**, *109*, 2185. Duarte, H.; Proynov, E.; Salahub, D. R. *J. Chem. Phys.* **1998**, *109*, 26.

[3] See for example: Knozinger, E.; Beichert, B. *J. Phys. Chem*. **1995**, *99*, 4906. Dutton, C.; Sazonor, A.; Beaudet, R. A. *J. Chem. Phys.* **1996**, *100*, 17772.

[4] See for example: Pubanz, G. A.; Maroncelli, M.; Nibler, J. W. *Chem. Phys. Lett*. **1985**, *120*, 313.

[5] See for example: Shafizadeh, N.; Brechignac, P.; Dyndgaard, M.; Fillion, J. H.; Gauyacq, D.; Levy, B.; Miller, J. C.; Pino, T.; Raoult, M. *J. Chem. Phys.* **1998**, *108*, 9313. Yan, J. S.; Yang, M. H.; Xie, D. Q. *J. Chem. Phys.* **1998**, *109*, 10284. Raducu, V.; Jasmin, D.; Dahoo, R.; Brosset, P.; Gauthier-Roy, B.; Abouaf-Marguin, L. *J. Chem. Phys.* **1995**, *102*, 9235.

[6] Ferguson, E. E.; Fehsenfeld, F. C.; Albritton, D. L. In *Gas-Phase Ion Chemistry*; Bowers, M. T., Ed.; Academic: NewYork, 1979; Vol. 1, p 45.

[7] Coe, J. V.; Snodgrass, J. T.; Freidhoff, C. B.; McHugh, K. M.; Bowen, K. H. *J. Chem. Phys.* **1987**, *87*, 4302. Posey, L. A.; Johnson, M. A. *J. Chem. Phys*. **1988**, *88*, 5383. Arnold, D. W.; Newmark, D. M. *J. Chem. Phys.* **1995**, *102*, 7035.

[8] Jacox, M. E.; Thompson, W. E. *J. Chem. Phys*. **1990**, *93*, 7609.

[9] Strobel, A.; Knoblanch, N.; Agreiter, J.; Smith, A. M.; Neider-Schatteburg, G.; Bondybey, V. E. *J. Phys. Chem*. **1995**, *99*, 872.

[10] Andrews, L.; Zhou, M. F.; Willson, S. P.; Kushto, G. P. *J. Chem. Phys.* **1998**, *109*, 177.

[11] Lugez, C. L.; Thompson, W. E.; Jacox, M. E.; Snis, A.; Panas, I. *J. Chem. Phys*. **1999**, *110*, 10345.

[12] DeLuca, M. J.; Niu, B.; Johnson, M. A. *J. Chem. Phys.* **1988**, *88*, 5857. Tsukuda, T.; Johnson, M. A.; Nagata, T. *Chem. Phys. Lett.* **1997**, *268*, 429.

[13] Fleischman, S. H.; Jordan, K. D. *J. Phys. Chem.* **1987**, *91*, 1300.

[14] Zhou, M. F.; Andrews, L. *J. Chem. Phys.* **1999**, *110*, 2414, 6820.

[15] Thompson, W. E.; Jacox, M. E. *J. Chem. Phys.* **1999**, *111*, 4487.

[16] Hiraoka, K; Yamabe, S. *J. Chem. Phys*. **1991**, *95*, 6800.

[17] See for example: Bondybey, V. E.; Smith, A. M.; Agreiter, J. *Chem. Rev.* **1996**, *96*, 2113 and references therein.

[18] Bondybey, V. E. *J. Phys. Chem.* **1982**, *86*, 3396.

[19] Bondybey, V. E.; English, J. H. *Chem. Phys. Lett*. **1984**, *111*, 195.

[20] Knight, L. B., Jr.; Earl, E.; Ligon, A. R.; Cobranchi, D. P.; Woodward, J. R.; Bostick, J. M.; Davidson, E. R.; Feller, D. *J. Am. Chem. Soc*. **1986**, *108*, 5065.

[21] Rasanen, M.; Liu, J. Y.; Dzugan, T. P.; Bondybey, V. E. *Chem. Phys. Lett*. **1987**, *142*, 308.

[22] Zhou, M. F.; Andrews, L. *J. Am. Chem. Soc.* **1998**, *120*, 11499.

[23] Zhou, M. F.; Andrews, L. *J. Am. Chem. Soc*. **1999**, *121*, 9171.

[24] Chen, M. H.; Wang, X. F.; Zhang, L. N.; Yu, M.; Qin, Q. Z. *Chem. Phys.* **1999**, *242*, 81.

10.1021/ja000041v CCC: $19.00

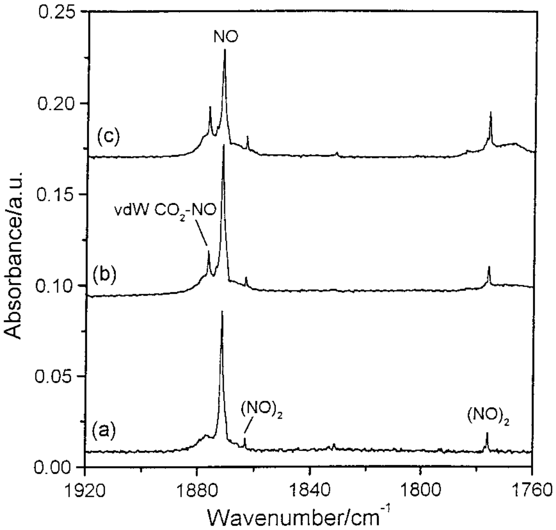

**Figure 1.** Infrared spectra in the 1920−1760 cm$^{-1}$ region from co-deposition of NO and $CO_2$ in excess argon at 11K: (a) 0.2% NO, (b) 0.2% NO + 0.5% $CO_2$, and (c) after 25 K annealing of sample (b).

The 1064 nm Nd:YAG laser fundamental (Spectra Physics, DCR 150, 20 Hz repetition rate and 8 ns pulse width) was focused onto a rotating metal target through a hole in a CsI window, and the ablated metal atoms and electrons were co-deposited with NO and $CO_2$ mixtures in excess argon onto a 11 K CsI window, which was mounted on a cold tip of a closed-cycle helium refrigerator (Air Products, Model CSW202) for 1−2 h at a rate of 2−4 mmol/h. Typically, 5−10 mJ/pulse laser power was used. Nitric oxide and carbon dioxide (Shanghai BOC, 99.99%) and isotopic $^{12}C^{16}O_2$ + $^{13}C^{16}O_2$ and $^{12}C^{16}O_2$ + $^{12}C^{16}O^{18}O$ + $^{12}C^{18}O_2$ mixtures (Cambridge Isotope Laboratories) were used in different experiments. Infrared spectra were recorded on a Bruker IFS113V spectrometer at 0.5 cm$^{-1}$ resolution using a DTGS detector.

Quantum chemical calculations were performed to predict the structure and vibrational frequencies of the $CO_2$−NO van der Waals complex and the $CO_2NO^-$ anion using the Gaussian 98 program.[26] The three parameter hybrid functional according to Becke with additional correlation corrections due to Lee, Yang, and Parr were utilized (B3LYP).[27,28] Additional comparison ab initio calculations were also done using the second-order Moller−Plesset perturbation theory (MP2) as well.[29] The 6-311+G(d), 6-311+G(2df), and aug-cc-PVDZ basis sets were used for C, N, and O atoms.[30,31] The geometries were fully optimized and vibrational frequencies calculated with analytic second derivatives.

## Results and Discussion

**Infrared Spectra.** Figure 1 shows the infrared absorption spectra of 0.2% NO in argon (trace a) and a mixture of 0.2% NO + 0.5% $CO_2$ in argon (trace b) in the region of the N−O stretching vibration. The NO/Ar spectrum reveals the strong NO absorption at 1871.8 cm$^{-1}$, and weak absorptions at 1863.3 and 1776.1 cm$^{-1}$ due to the symmetric and antisymmetric N−O stretching vibrations of the *cis*-$(NO)_2$. New absorption at 1876.5 cm$^{-1}$ was observed in the NO/$CO_2$/Ar spectrum, annealing to 25 K decreased the NO absorption at 1871.8 cm$^{-1}$ and increased the *cis*-$(NO)_2$ absorptions and the 1876.5 cm$^{-1}$ absorption (trace c in Figure 1).

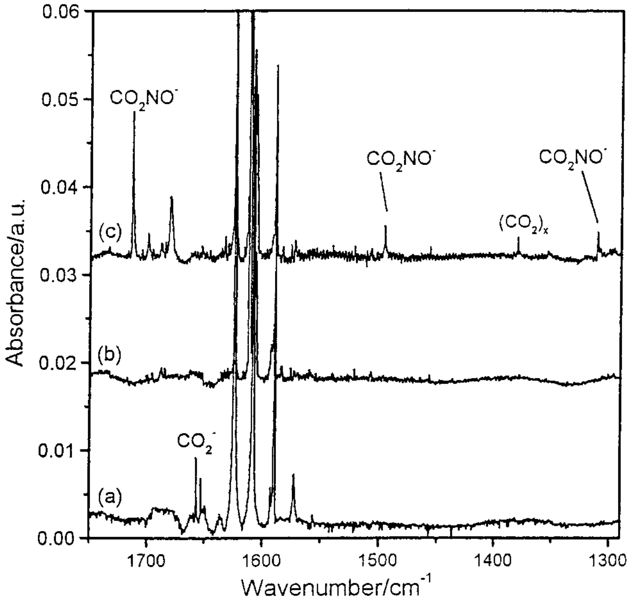

**Figure 2.** Infrared spectra in the 1750−1290 cm$^{-1}$ region from co-deposition of laser-ablated Ag with different samples: (a) 0.2% $CO_2$, (b) 0.1% NO, and (c) 0.1% NO + 0.2%$CO_2$.

**Table 1.** Metal Independent Absorptions (cm$^{-1}$) from Co-deposition of Laser-Ablated Metal with $CO_2$/NO/Ar Mixtures at 11 K

| $^{12}C^{16}O_2$ | $^{13}C^{16}O_2$ | $^{12}C^{16}O^{18}O$ | $^{12}C^{18}O_2$ | assignment |
|---|---|---|---|---|
| 1876.5 | | | | $CO_2$−NO N−O str |
| 1713.6 | 1666.0 | 1698.4 | 1682.3 | $CO_2NO^-$ asy-$CO_2$ |
| 1495.8 | 1494.8 | | 1494.8 | $CO_2NO^-$ N−O str |
| 1310.4 | 1292.2 | 1289.8 | 1270.7 | $CO_2NO^-$ sym-$CO_2$ |

Laser ablation experiments were done using the Pd and Ag metal targets with different NO and $CO_2$ concentrations, and the metal-independent absorptions are listed in Table 1. Figure 2 shows spectra in the 1750−1290 cm$^{-1}$ region using an Ag target with different samples in excess argon. After 1 h sample deposition at 11 K, the $CO_2^-$ anion absorption at 1657.0 cm$^{-1}$ and the $(CO_2^-)(CO_2)_x$ complex absorption at 1652.8 cm$^{-1}$ were observed in this spectral region using 0.2% $CO_2$ in argon, as shown in trace (a). Trace (b) shows the spectrum with 0.1% NO in argon, and sample deposition reveals the $NO_2$ absorption at 1610.8 cm$^{-1}$. Trace (c) shows the spectrum using a 0.1% NO + 0.2%$CO_2$ mixed sample; new absorptions were observed at 1713.6, 1495.8, and 1310.4 cm$^{-1}$, but the $CO_2^-$ and $(CO_2^-)(CO_2)_x$ absorptions were eliminated.

Similar experiments were done using a Pd target, and representative spectra in the 1740−1290 cm$^{-1}$ region are shown in Figure 3. When the NO/Ar sample was used, no distinctive absorptions were observed in this region except those of $H_2O$ and $NO_2$ absorption at 1610.8 cm$^{-1}$ [trace (a)]. The bands at 1713.6, 1495.8, and 1310.4 cm$^{-1}$ were observed again after deposition with a 0.1% NO + 0.2% $CO_2$ sample [trace (b)]. These three bands were destroyed upon 20 min of photolysis with a 355 nm laser beam [trace (c)] and could not be

---

(25) Burkholder, T. R.; Andrews, L. *J. Chem. Phys.* **1991**, *95*, 8697.

(26) Frisch, M. J.; Trucks, G. W.; Schlegel, H. B.; Scuseria, G. E.; Robb, M. A.; Cheeseman, J. R.; Zakrzewski, V. G.; Montgomery, J. A., Jr.; Stratmann, R. E.; Burant, J. C.; Dapprich, S.; Millam, J. M.; Daniels, A. D.; Kudin, K. N.; Strain, M. C.; Farkas, O.; Tomasi, J.; Barone, V.; Cossi, M.; Cammi, R.; Mennucci, B.; Pomelli, C.; Adamo, C.; Clifford, S.; Ochterski, J.; Petersson, G. A.; Ayala, P. Y.; Cui, Q.; Morokuma, K.; Malick, D. K.; Rabuck, A. D.; Raghavachari, K.; Foresman, J. B.; Cioslowski, J.; Ortiz, J. V.; Baboul, A. G.; Stefanov, B. B.; Liu, G.; Liashenko, A.; Piskorz, P.; Komaromi, I.; Gomperts, R.; Martin, R. L.; Fox, D. J.; Keith, T.; Al-Laham, M. A.; Peng, C. Y.; Nanayakkara, A.; Gonzalez, C.; Challacombe, M.; Gill, P. M. W.; Johnson, B.; Chen, W.; Wong, M. W.; Andres, J. L.; Gonzalez, C.; Head-Gordon, M.; Replogle, E. S.; Pople, J. A. *Gaussian 98*, Revision A.7; Gaussian, Inc.: Pittsburgh, PA, 1998.

(27) Lee, C.; Yang, E.; Parr, R. G. *Phys. Rev. B* **1988**, *37*, 785.

(28) Becke, A. D. *J. Chem. Phys.* **1993**, *98*, 5648.

(29) Moller, C.; Plesset, M. S. *Phys. Rev. B* **1984**, *46*, 618.

(30) McLean, A. D.; Chandler, G. S. *J. Chem. Phys.* **1980**, *72*, 5639.

(31) Krishnan, R.; Binkley, J. S.; Seeger, R.; Pople, J. A. *J. Chem. Phys.* **1980**, *72*, 650.

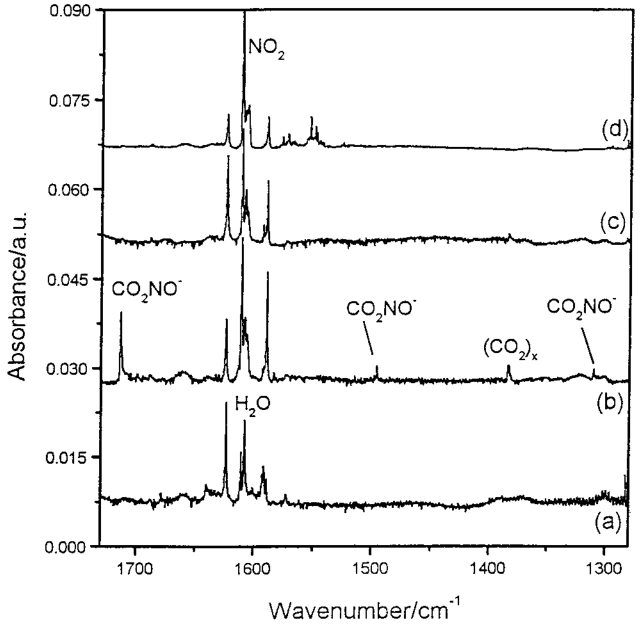

**Figure 3.** Infrared spectra in the 1740−1290 cm$^{-1}$ region from co-deposition of laser-ablated Pd with different samples: (a) 0.1% NO, (b) 0.1% NO + 0.2% $CO_2$, (c) after 20 min of 355 nm photolysis of sample (b), and (d) 0.1% NO + 0.2% $CO_2$ + 0.04% $CCl_4$.

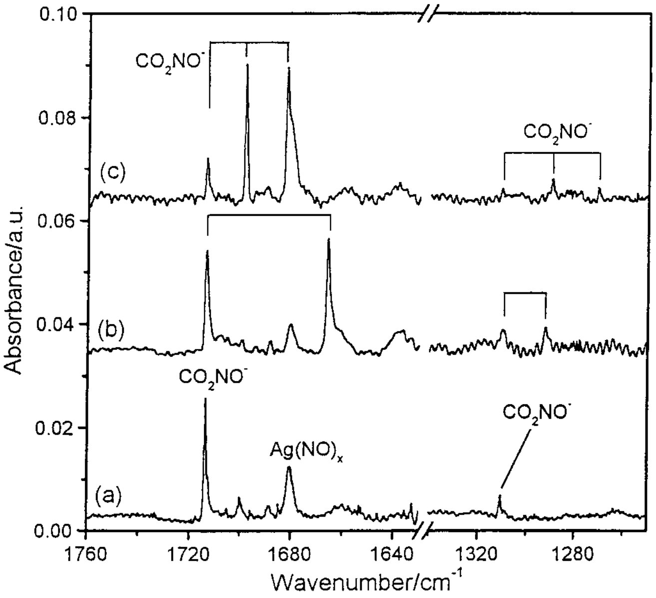

**Figure 4.** Infrared spectra in the 1760−1630 and 1340−1250 cm$^{-1}$ regions from co-deposition of laser-ablated Ag with different samples: (a) 0.1% NO + 0.2% $CO_2$, (b) 0.1% NO + (0.3% $^{12}C^{16}O_2$ + 0.3%$^{13}C^{16}O_2$), and (c) 0.1% NO + (0.125% $^{12}C^{16}O_2$ + 0.25% $^{12}C^{16}O^{18}O$ + 0.125% $^{12}C^{18}O_2$).

reproduced on further annealing to 25 K. Trace (d) shows the spectrum using the same experimental conditions as spectrum (b) with 0.04% $CCl_4$ added to serve as an electron trap; the spectrum showed that the 1713.6, 1495.8, and 1310.4 cm$^{-1}$ bands were totally eliminated.

Experiments were also done using isotopically labeled samples, and the results are shown in Figure 4. In the mixed 0.2% NO + (0.3% $^{12}C^{16}O_2$ + 0.3% $^{13}C^{16}O_2$) experiments, doublets at 1713.6 and 1666.0 cm$^{-1}$, 1495.8 and 1494.8 cm$^{-1}$, 1310.4 and 1292.2 cm$^{-1}$ were produced for the 1713.6, 1495.8, and 1310.4 cm$^{-1}$ bands [trace (b)]. In the mixed 0.2% NO + (0.125% $^{12}C^{16}O_2$ + 0.25% $^{12}C^{16}O^{18}O$ + 0.125% $^{12}C^{18}O_2$) experiments [trace (c)], the triplet at 1713.6, 1698.4, and 1682.3 cm$^{-1}$ was produced for the upper mode and the triplet at 1310.4, 1289.8, and 1270.7 cm$^{-1}$ was produced for the lower mode. It should be mentioned that in Figure 4c, a broad band at 1680 cm$^{-1}$ contributes to the absorption at 1682.3 cm$^{-1}$. The 1680 cm$^{-1}$ band was presented in the Ag + NO/Ar experiments, suggesting that it is a reaction product of Ag and NO, and is most likely due to the N−O stretching vibration of an $Ag(NO)_x$ molecule. It should be noted that there is no obvious metal-dependent absorption in the experiments using Pd as the target.

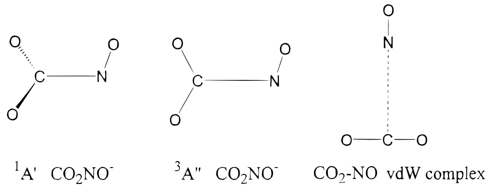

**Figure 5.** Structures of the $CO_2NO^-$ anion and the $CO_2$−NO van der Waals complex. For the $^1$A′ $CO_2NO^-$, the CNO plane is perpendicular to the OCO plane. The $^3$A″ $CO_2NO^-$ has planar structure.

**Calculation Results.** B3LYP and MP2 calculations were first done on $CO_2$, NO neutral molecules, and their anions. The $CO_2$ bond length was estimated to be between 1.160 and 1.170 Å, very close to the 1.160 Å experimental value.[32] The $CO_2^-$ anion was predicted to have a bond length lie between 1.229 and 1.238 Å and a bond angle within 137 to 138°, which are in good agreement with higher level CCSD(T)/aug-cc-PVTZ calculations.[33] The B3LYP calculations gave 1.148, 1.146, and 1.154 Å bond lengths for NO in the 6-311+G(d), 6-311+G(2df), and aug-cc-PVDZ basis sets, respectively, which are in excellent agreement with the experimental value of 1.151 Å;[34] the MP2 bond length 1.135 Å is slightly shorter than the experimental value; however, the B3LYP and MP2 bond lengths for the $NO^-$ ($^3\Sigma^-$) (1.262−1.266 Å) are consistent with each other.

Theoretical calculations were performed on the $CO_2$−NO van der Waals complex, and one stable structure was found, as shown in Figure 5. The calculated geometric parameters and vibrational frequencies are listed in Table 2. The $CO_2$−NO complex was predicted to have a T-shaped structure with the NO monomer along the $C_2$ symmetry axis of the $CO_2$ moiety and the N atom facing to the C atom. The distance between the N and C atoms was predicted to be between 3.1 and 3.3 Å at all levels of theory employed here.

Theoretical calculations were done on the $CO_2NO^-$ anion, and one stable minimum was found on both the singlet and triplet potential energy surfaces, as shown in Figure 5. The calculated geometric parameters and vibrational frequencies are listed in Tables3 and 4, respectively. As can be seen excellent agreement is found between the B3LYP hybrid density functional theory and the second-order Moller−Plesset perturbation theory. The calculated vertical detachment energy, adiabatic electron affinity, and dissociation energies with respect to $CO_2$ + $NO^-$ or $CO_2^-$ + NO are listed in Table 5.

The $^1$A′ state $CO_2NO^-$ anion is coordinated between the C and N atoms and has a nonplanar structure with $C_s$ symmetry, with the CNO plane perpendicular to the OCO plane. At the B3LYP/6-311+G(d) level of theory, the C−N bond distance is 1.514 Å and the N−O bond distance is 1.219 Å. The unpaired electron in the $\pi^*$ orbital of free NO is used to form a covalent

---

[32] Teffo, J. L.; Sulakshina, O. N.; Perevalo, V. I. *J. Mol. Struct.* **1992**, *156*, 48.

[33] Knight, L. B., Jr.; Hill, D.; Berry, K.; Babb, R.; Feller, D. *J. Chem. Phys.* **1996**, *105*, 5672.

[34] Huber, K. P.; Herzberg, G. *Molecular Spectra and Molecular Structure Constants of Diatomic Molecules*; Van Nostrand: New York, 1979.

**Table 2.** Calculated Energies (hartrees), Geometries (Å, deg), Vibrational Frequencies ($cm^{-1}$), and Intensities (km/mol) for the $CO_2$−NO van der Waals Complex at Various Levels

| | B3LYP/6-311+G(d) | B3LYP/6-311+G(2df) | B3LYP/aug-cc-PVDZ | MP2/6-311+G(d) |
|---|---|---|---|---|
| *E* | −318.579150 | −318.596129 | −318.528095 | −317.833640 |
| C−N | 3.271 | 3.305 | 3.266 | 3.121 |
| N−O | 1.147 | 1.145 | 1.153 | 1.133 |
| C−O | 1.161 | 1.160 | 1.167 | 1.170 |
| ∠OCO | 179.6 | 179.7 | 179.7 | 179.7 |
| OCO asym str | 2418.2(696) | 2405.9(667) | 2387.5(636) | 3621.4(2074) |
| NO str | 1984.7(49) | 1975.5(47) | 1980.1(46) | 2433.3(586) |
| OCO sym str | 1373.1(0) | 1371.4(0) | 1354.6(0) | 1335.9(0) |
| OCO bending | 668.3(33) | 678.6(29) | 667.0(27) | 654.8(24) |
| OCO bending | 664.0(45) | 673.9(42) | 663.3(39) | 652.3(34) |
| out-of-plane wag | 59.7(0) | 52.8(0) | 69.4(0) | 84.8(0) |
| N−C str | 42.3(0) | 37.4(0) | 42.2(0) | 57.8(0) |
| NO wag | 19.8(0) | 16.8(0) | 20.1(0) | 10.8(0) |
| torsion | 9.7(0) | 6.7(0) | 17.9(0) | 26.8i(0.2) |

**Table 3.** Calculated Energies (hartrees), Geometries (Å, deg), Vibrational Frequencies ($cm^{-1}$), and Intensities (km/mol) for the $^1A'$ $CO_2NO^-$ Anion at Various Levels

| | B3LYP/6-311+G(d) | B3LYP/6-311+G(2df) | B3LYP/aug-cc-PVDZ | MP2/6-311+G(d) |
|---|---|---|---|---|
| *E* | −318.625586 | −318.640855 | −318.577470 | −317.859772 |
| C−N | 1.514 | 1.508 | 1.510 | 1.516 |
| N−O | 1.219 | 1.217 | 1.224 | 1.232 |
| C−O | 1.238 | 1.236 | 1.244 | 1.243 |
| ∠CNO | 114.5 | 114.7 | 114.2 | 112.4 |
| ∠OCO | 134.6 | 134.5 | 134.4 | 135.0 |
| OCO asym str | 1743.9(633) | 1735.9(605) | 1726.0(591) | 1778.3(725) |
| NO str | 1561.5(196) | 1559.4(184) | 1563.7(180) | 1507.1(44) |
| OCO sym str | 1333.5(141) | 1337.6(136) | 1328.9(129) | 1339.8(171) |
| C−N str | 911.7(11) | 916.7(12) | 909.6(10) | 924.7(4) |
| OCO bending | 789.7(28) | 795.8(26) | 787.4(22) | 815.5(45) |
| OCO bending | 549.1(12) | 551.1(12) | 550.6(13) | 568.2(10) |
| NO wag | 340.4(9) | 340.4(8) | 339.0(8) | 344.0(8) |
| Out-of-plane wag | 329.5(1) | 325.3(0.8) | 324.9(0.7) | 364.7(4) |
| torsion | 142.2(0) | 147.4(0) | 148.0(0) | 102.1(0.3) |

**Table 4.** Calculated Energies (hartrees), Geometries (Å, deg), Vibrational Frequencies ($cm^{-1}$), and Intensities (km/mol) for the $^3A''$ $CO_2NO^-$ Anion at Various Levels

| | B3LYP/6-311+G(d) | B3LYP/6-311+G(2df) | B3LYP/aug-cc-PVDZ | MP2/6-311+G(d) |
|---|---|---|---|---|
| *E* | −318.61870 | −318.633312 | −318.568770 | −317.841077 |
| C−N | 1.849 | 1.845 | 1.781 | 1.814 |
| N−O | 1.226 | 1.223 | 1.230 | 1.232 |
| C−O | 1.206 | 1.204 | 1.217 | 1.212 |
| ∠CNO | 120.6 | 120.5 | 121.2 | 120.5 |
| ∠OCO | 143.9 | 143.9 | 141.8 | 144.1 |
| OCO asym str | 1984.1(721) | 1976.6(699) | 1925.3(672) | 2013.3(728) |
| N−O str | 1554.2(116) | 1552.3(112) | 1561.0(94) | 1636.3(138) |
| OCO sym str | 1275.0(313) | 1275.1(299) | 1260.6(280) | 1285.3(298) |
| OCO bending | 680.6(22) | 684.1(19) | 680.7(18) | 704.2(208) |
| OCO bending | 669.2(253) | 664.7(240) | 663.0(202) | 699.4(16) |
| NO wag | 452.5(8) | 449.0(8) | 468.0(9) | 487.1(44) |
| C−N str | 251.4(24) | 248.4(21) | 258.6(22) | 248.3(19) |
| $CO_2$ wag | 172.8(110) | 168.6(114) | 188.1(125) | 264.9(149) |
| torsion | 101.5(0) | 102.1(0) | 102.4(0) | 115.5(0) |

bond with C and the N rehybridizes from sp to $sp^2$. As a result, the C−N bond is a single bond, while the N−O bond becomes a double bond as evident from the longer N−O bond length versus free NO. The charge is delocalized, with about 0.3e located on the NO moiety and 0.7e located on the $CO_2$ moiety. The dissociation energies with respect to separated $CO_2 + NO^-$ or $CO_2^- + NO$ were predicted to be 21−25 and 38−42 kcal/mol, respectively, without zero-point energy correction. This anion can be viewed as forming from electron capture by the T-shaped $CO_2$−NO van der Waals complex; as listed in Table 5, the adiabatic electron affinity was predicted to be around 1.2 eV at the B3LYP levels.

**Table 5.** Vertical Detachment Energy (VDE, eV), Dissociation Energy ($D_0$, kcal/mol) with Respect to $CO_2 + NO^-$ and $CO_2^- +$ NO, and the Adiabatic Electron Affinity ($E_a$, eV) Calculated at Various Levels (values after zero-point energy corrections are listed in parentheses)

| | VDE | $D_0$ | | $E_a$ |
|---|---|---|---|---|
| B3LYP/6-311+G(d) | 3.6 | 21.0 (19.3)[a] | 38.1(35.1)[b] | 1.26(1.24) |
| B3LYP/6-311+G(2df) | 3.6 | 21.2(19.6) | 38.1(35.1) | 1.22(1.19) |
| B3LYP/aug-cc-PVDZ | 3.6 | 22.6(20.9) | 39.2(36.2) | 1.34(1.31) |
| MP2/6-311+G(d) | 4.8 | 25.3(23.6) | 41.6(40.8) | 0.71(0.78) |

[a] Calculated with respect to $CO_2 + NO^-$. [b] Calculated with respect to $CO_2^- +$ NO.

The $^3A''$ $CO_2NO^-$ anion is also coordinated between N and C atoms, but has a planar structure with $C_s$ symmetry. It was predicted to be 4.3−5.5 kcal/mol higher in energy than the $^1A'$ state at the B3LYP levels, and the energy difference was predicted to be 11.7 kcal/mol at the MP2 level. The C−N bond distance was predicted to be much longer than that of the $^1A'$ state. At the B3LYP/6-311+G(d) level of theory, the C−N bond distance is 1.849 Å. In this case, the N does not rehybridize and the two unpaired electrons reside in two orbitals formed mainly from the NO $\pi^*$ orbitals, and can be viewed as a $CO_2^-$−$NO^-$ complex. The $^3A''$ state $CO_2NO^-$ was predicted to have a shorter C−O bond distance and a more open OCO bond angle.

**$CO_2$−NO Complex.** The 1876.5 $cm^{-1}$ band is assigned to a $CO_2$−NO van der Waals complex based on theoretical calculations. It is only 4.7 $cm^{-1}$ blue-shifted from the NO absorption at 1871.8 $cm^{-1}$, and is produced with mixed NO + $CO_2$ deposit only. The assignment is strongly supported by theoretical calculations. The N−O stretching vibration of the $CO_2$−NO complex was predicted to be blue-shifted by 4.3, 5.4, and 6.0 $cm^{-1}$, respectively, with respect to the calculated N−O stretching vibration of the free NO molecule at the B3LYP/6-311+G-(d), B3LYP/6-311+G(2df), and B3LYP/aug-cc-PVDZ levels of theory. The $CO_2$ antisymmetric stretching vibration of the $CO_2$−NO complex was predicted to be red-shifted by 2.6, 0.8, and 1.1 $cm^{-1}$, respectively, with respect to the free $CO_2$ molecule. This mode was overlapped by the strong $CO_2$ absorption and could not be resolved here.

**$CO_2NO^-$**. The 1713.6, 1495.8, and 1310.4 $cm^{-1}$ bands tracked through all the experiments, suggesting different vibrational modes of the same molecule. The 1713.6 $cm^{-1}$ band is strong, while the other two bands are much weaker. These three bands were only produced in the mixed NO + $CO_2$ experiments indicating that both NO and $CO_2$ units are involved in this species. The band positions observed with different metal targets remain to within 0.1 $cm^{-1}$ unshifted, suggesting that this species is metal independent and is due to reaction product involving the common reagents, namely electrons produced in the laser ablation process and the NO and $CO_2$ molecules. The 1713.6 $cm^{-1}$ band shifted to 1666.0 and 1682.3 $cm^{-1}$ using the $^{13}C^{16}O_2$ and $^{12}C^{18}O_2$ samples and gave 12/13 and 16/18 isotopic ratios of 1.0286 and 1.0186, respectively, which are characteristic of an antisymmetric OCO stretching vibration. The doublet structure in the mixed $^{12}C^{16}O_2$ + $^{13}C^{16}O_2$ spectrum and triplet in the mixed $^{12}C^{16}O_2$ + $^{12}C^{16}O^{18}O$ + $^{12}C^{18}O_2$ spectrum indicated that one $CO_2$ unit with two equivalent O atoms is involved in this vibrational mode. The weak 1310.4 $cm^{-1}$ band shifted to 1292.2 $cm^{-1}$ with $^{13}C^{16}O_2$ and to 1270.7 $cm^{-1}$ with $^{12}C^{18}O_2$, and gave a small 12/13 isotopic ratio of 1.0141 and a large 16/18 isotopic ratio of 1.0312, which are characteristic of a symmetric OCO stretching vibration. The mixed $^{12}C^{16}O_2$ + $^{13}C^{16}O_2$ spectrum showed a doublet and the mixed $^{12}C^{16}O_2$ + $^{12}C^{16}O^{18}O$ + $^{12}C^{18}O_2$ spectrum showed a triplet with approximately 1:2:1 relative intensities, indicating that one C atom and two equivalent O atoms are involved in this vibrational mode. The 1495.8 $cm^{-1}$ band exhibited very small shift when isotopic $CO_2$ samples were used, suggesting that this band is mainly a N−O stretching vibration and is slightly coupled by the $CO_2$ unit. Accordingly, this species involves one NO and one $CO_2$ units, and has the formula $NCO_3$. The photosensitive behavior and its reduction in $CCl_4$ doping experiments strongly suggest an anion assignment. Therefore, the 1713.6, 1495.8, and 1310.4 $cm^{-1}$ bands are assigned to the antisymmetric OCO stretching, N−O stretching, and symmetric OCO stretching vibrations of the $CO_2NO^-$ anion.

**Table 6.** Observed and B3LYP/6-311+G(d) Calculated Isotopic Frequency Ratios for the $^1A'$ $CO_2NO^-$ Anion

| | $^{12}C^{16}O_2/^{13}C^{16}O_2$ | | $^{12}C^{16}O/^{12}C^{18}O_2$ | |
|---|---|---|---|---|
| mode | calcd | obsd | calcd | obsd |
| asym-$CO_2$ | 1.0274 | 1.0286 | 1.0181 | 1.0186 |
| N−O str | 1.0001 | 1.0074 | 1.0001 | 1.0074 |
| sym-$CO_2$ | 1.0148 | 1.0141 | 1.0355 | 1.0312 |

**Table 7.** Geometric Parameters (Å, deg), Dissociation Energies (kcal/mol), and Mulliken Charge Populations Calculated at the B3LYP/6-311+G(d) Level and the Observed Antisymmetric $CO_2$ Stretching Vibrational Frequencies ($cm^{-1}$) for the $CO_2^-XO^-$(X = C, N, O) Anions

| | $C_2O_3^-$ | $CO_2NO^-$ | $CO_4^-$ |
|---|---|---|---|
| C−X | 1.617 | 1.514 | 1.704 |
| X−O | 1.190 | 1.219 | 1.317 |
| C−O | 1.237 | 1.238 | 1.209 |
| ∠CXO | 125.4 | 114.5 | 112.1 |
| ∠OCO | 134.8 | 134.6 | 142.4 |
| $D_0{}^a$ | 11.7 | 19.3 | 18.8 |
| $Q_{X-O}$ | −0.33 | −0.28 | −0.45 |
| $\upsilon_{\text{asym}-CO_2}$ | 1701.7 | 1713.6 | 1891.5 |

[a] After zero-point energy corrections.

The $CO_2NO^-$ anion assignment is further confirmed by theoretical calculations. As has been mentioned, the present theoretical calculations predicted that the $CO_2NO^-$ anion has a $^1A'$ ground state with the antisymmetric OCO stretching, N−O stretching, and symmetric OCO stretching vibrational frequencies at 1743.9, 1561.5, and 1333.5 $cm^{-1}$ at the B3LYP/6-311+G(d) level, which must be scaled by 0.983, 0.958, and 0.983 to match the observed values; these scale factors are appropriate for this level of theory.[35] The calculated intensity distribution (633:196:141) is in excellent agreement with observed relative intensities. The observed and calculated isotopic frequency ratios for these three modes at the B3LYP/6-311+G(d) level are presented in Table 6; the calculated ratios are in reasonable agreement with the observed ratios.

It is interesting to compare the $CO_2NO^-$ anion with the $C_2O_3^-$ anion recently reported in our group[36] and the $CO_4^-$ anion reported previously.[37] Table 7 lists the geometric parameters, dissociation energies, charge distributions calculated at the B3LYP/6-311+G(d) level, and the observed antisymmetric $CO_2$ stretching vibrational frequency for these three anions. All three anions have very similar structure and are covalently bonded molecules. The $CO_4^-$ anion has a slightly more open OCO bond angle, and a higher antisymmetric $CO_2$ stretching vibrational frequency. It is well-known that calculations on molecular anions are more difficult than those on neutral species; however, B3LYP calculations predicted the dissociation energies of anions such as $CO_4^-$ and $FCO_2^-$ quite well. The dissociation energies of $CO_4^-$ and $FCO_2^-$ with respect to $CO_2$ + $O_2^-$ and $F^-$ + $CO_2$ were predicted to be 18.8 and 30.8 kcal/mol at the B3LYP/6-311+G(d) level, after zero-point energy corrections,[38] slightly lower than the experimental values of 21 and 32.3 kcal/mol.[39,40] The dissociation energies of $C_2O_3^-$ and $CO_2NO^-$ with respect to $CO_2^-$ + CO and $CO_2$ + $NO^-$ were predicted to be 11.7 and 19.3 kcal/mol, respectively; taking the $CO_4^-$ and $FCO_2^-$ as a criterion, we expect the experimental dissociation energies will be about 2 kcal/mol higher than the calculated values.

The $CO_2NO^-$ anion is isoelectronic with $N_2O_3$ and $CO_4$. The $CO_4$ neutral is predicted to be a weakly bound $O_2C$−$O_2$ van

---

[35] Bytheway, I.; Wong, M. W. *Chem. Phys. Lett.* **1998**, *282*, 219.

[36] Zhou, M. F.; Zhang, L. N.; Cheng, M. H.; Qin, Q. Z. *J. Chem. Phys.* in press.

[37] Jacox, M. E.; Thompson, W. E. *J. Phys. Chem.* **1991**, *95*, 2781.

[38] At the B3LYP/6-311+G(d) level, the calculated geometry parameters for the $^1A_1$ $FCO_2^-$ are as follows: $R_{CF}$ = 1.521 Å, $R_{CO}$ = 1.219 Å, ∠OCO = 138.2°.

[39] Fehsenfeld, F. C.; Albritton, D. L.; Streit, G. E.; Davidson, J. A.; Howard, C. J.; Ferguson, E. E. *Atmos. Environ.* **1977**, *11*, 283.

[40] Hiraoka, K.; Mizuse, S.; Yamabe, S. *J. Chem. Phys.* **1987**, *87*, 3647.

der Waals complex with T-shaped geometry. The $O_2C-OO$ distance is predicted to be 3.704 Å at the B3LYP/6-311+G(d) level. This $O_2C-O_2$ complex is comparable to the $^3A''$ $O_2C-NO^-$ anion complex, but the $^3A''$ $O_2C-NO^-$ is more strongly bound than the $O_2C-O_2$ complex due to electrostatic interaction. The most stable structure of the $N_2O_3$ neutral is planar asym-$N_2O_3$ coordinated between two N atoms, that is, the two radical electrons combine and form a covalent bond.[41] The asym-$N_2O_3$ neutral and the $^1A'$ $CO_2NO^-$ anion are more strongly bound than the $O_2C-O_2$ complex due to covalent bonding character.

It is well-known that laser ablation of a metal target produces a plume that contains metal atoms, cations, and electrons. In our experiments, pulsed laser ablation is combined with the conventional continuous spray matrix gas deposition, in which the laser-ablated plume was expanded into a gas stream of a $CO_2$ and NO mixture in excess argon. Since the density of atoms and electrons in the plume is high, interaction between the expanding plume and ambient gas molecules could lead to a variety of new molecules and ions. As the formation of the $CO_2NO^-$ anion does not depend on metal targets, the ablated metal atoms themselves do not play a role in the formation of the anion. The metal cations are the most likely counterions to provide the electroneutrality of the solid deposit, as no molecular cation is identified in the product infrared spectra.

There are three possible reactions to form the $CO_2NO^-$ anion. Since the neutral $CO_2-NO$ van der Waals complex is stable and is observed in our experiments, the $CO_2NO^-$ anion is expected to be formed via electron capture by this neutral $CO_2-NO$ van der Waals complex, i.e., reaction 1, which was calculated to be exothermic by about 27−29 kcal/mol at the B3LYP levels of theory. The $CO_2NO^-$ anion can also be produced by ion−molecule reactions 2 and 3, which were predicted to be exothermic.

$$CO_2-NO + e^- \rightarrow CO_2NO^- \quad \Delta E = -28.5\,\text{kcal/mol} \quad (1)$$

$$CO_2 + NO^- \rightarrow CO_2NO^- \quad \Delta E = -19.3\,\text{kcal/mol} \quad (2)$$

$$CO_2^- + NO \rightarrow CO_2NO^- \quad \Delta E = -35.1\,\text{kcal/mol} \quad (3)$$

The $CO_2NO^-$ absorptions decreased on annealing, suggesting that reactions 1−3 do not proceed in an argon matrix, and the $CO_2NO^-$ anion are mainly formed in the gas phase or on the surface of the solid deposit during co-condensation.

It is interesting to note that the $CO_2^-$ anion absorption was observed in the pure $CO_2$/Ar experiments, but was not present in the mixed $CO_2$ + NO experiments. Weak $NO_2^-$ and $(NO)_2^-$ anion absorptions were observed.[13,42] The $NO^-$ is a very weak infrared absorber, and the vibrational fundamental of ground-state $NO^-$ has not been definitively established in either the gas phase or matrices. The alkali metal atom−nitric oxide molecule reaction products $M^+NO^-$ were observed at 1353−1374 $cm^{-1}$ for $Li^+$ to $Cs^+$ in solid argon.[43] Most of the gas-phase electron scattering work has given $NO^-$ frequency values in this region with fairly large uncertainty,[44] but a recent vibrational autodetachment study reported a lower 1284 ± 10 $cm^{-1}$ value.[45] There is no obvious absorption in this region that can be assigned to the $NO^-$ anion.

## Conclusions

Matrix-isolation FTIR combined with theoretical calculations has been employed to identify a new $CO_2NO^-$ anion for the first time. This anion is generated by laser ablation of transition metal targets with concurrent 11 K deposition of $NO/CO_2/Ar$ mixtures. Based on isotopic substitution and theoretical calculations, the major observed bands in the IR spectra can be assigned to the antisymmetric $CO_2$ stretching, N−O stretching, and symmetric $CO_2$ stretching vibrations of the $CO_2NO^-$ anion. The anion assignment was further supported by photolysis and $CCl_4$ doping experiments. Our theoretical calculation results show that the $CO_2NO^-$ anion is a covalently bound molecule with coordination between the C and N atoms. The binding energy of $CO_2NO^-$ with respect to $CO_2 + NO^-$ is estimated to be about 21−22 kcal/mol, comparable to that of the $CO_4^-$ anion, and is higher than those of the $C_2O_4^-$ and $C_2O_3^-$ anions. Our experimental results showed that laser ablation of transition metal targets is a powerful technique to produce metal-independent new anions via electron capture of neutral intermediates and free radicals during laser ablation.

**Acknowledgment.** This work was supported by the 973 project of China.

JA000041V

---

(41) See for example: Bibart, C. H.; Ewing, G. E. *J. Chem. Phys*. **1974**, *61*, 1293.

(42) Forney, D.; Thompson, W. E.; Jacox, M. E. *J. Chem. Phys.* **1993**, *99*, 7393.

(43) Milligan, D. E.; Jacox, M. E. *J. Chem. Phys.* **1971**, *55*, 3404. Tevault, D. E.; Andrews, L. *J. Phys. Chem*. **1973**, *77*, 1646.

(44) See for example: Zecca, A.; Lazzizzera, I.; Krauss, M.; Kuyatt, C. E. *J. Chem. Phys*. **1974**, *61*, 4560.

(45) Maricq, M. M.; Tanguay, N. A.; O'Brien, J. C.; Rodday, S. M.; Rinden, E. *J. Chem. Phys*. **1989**, *90*, 3136 and references therein.